# Probing the Properties of the Pulsar Wind in the Gamma-Ray Binary HESS J0632+057 with NuSTAR and VERITAS Observations

**Submitted to ApJ**
**PoS(ICRC2019)767 [arXiv:1908.03083]**

Raul R. Prado*[1], for the VERITAS Collaboration[†]
Charles Hailey[2], Shifra Mandel[2], Kaya Mori[2] (NuSTAR Collaboration[‡])

Variable Galactic Gamma-Ray Sources V, Barcelona, Sept. 4th – 6th, 2019

* raul.prado@desy.de
[1] Deutsches Elektronen-Synchrotron (DESY), Platanenallee 6, 15738 Zeuthen, Germany
[2] Columbia Astrophysics Laboratory, Columbia University, New York, NY 10027, USA
[†] https://veritas.sao.arizona.edu [‡]https://www.nustar.caltech.edu

HELMHOLTZ RESEARCH FOR GRAND CHALLENGES

NuSTAR VERITAS DESY.

# Overview

## HESS J0632+057

- $P_{orb}$ ~ 315 – 320 days
- d = 1.1 – 1.7 kpc
- Companion star MWC 148: B0ep
- Unknown nature of compact object
- Weak MeV – GeV detection Li et al. 2017
- Two orbital solutions available

Casares et al. 2012; Moritani et al. 2018

- See also Daniela's talk

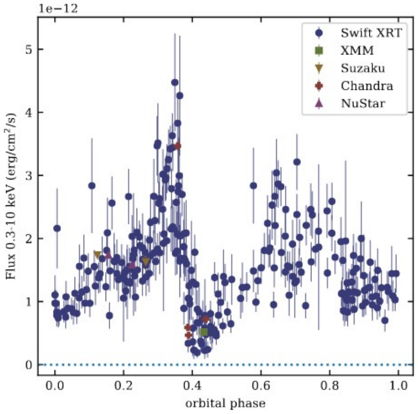


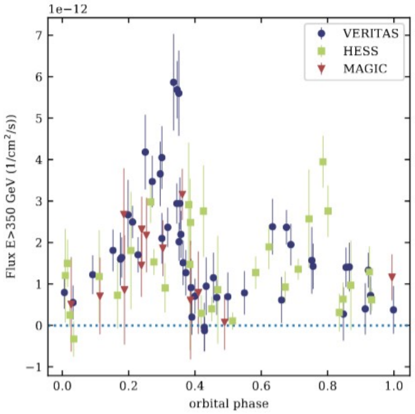


## Outline

### Observations and Data Analysis

- Combined observations by NuSTAR and VERITAS
- Nov. and Dec. 2017
- X-rays timing analysis
- TeV and X-rays spectral analysis

### System Parameters and Orbital Solutions

- Two orbital solutions, one of which is marginally compatible with the pulsar scenario.

### Modeling

- SED model fitting
- Probing the pulsar scenario: non-thermal emission from electron pair accelerated at the pulsar-wind termination shock.
- Observation well described by the model
- Constraints on pulsar wind magnetization

# Observations and Data Analysis

## NuSTAR

- Spectral resolution of 400 eV FWHM
- Absolute (relative) timing accuracy of 3 msec (10 μsec)
- Energy range: 3 – 79 keV
- Little to no dependence with $N_H$

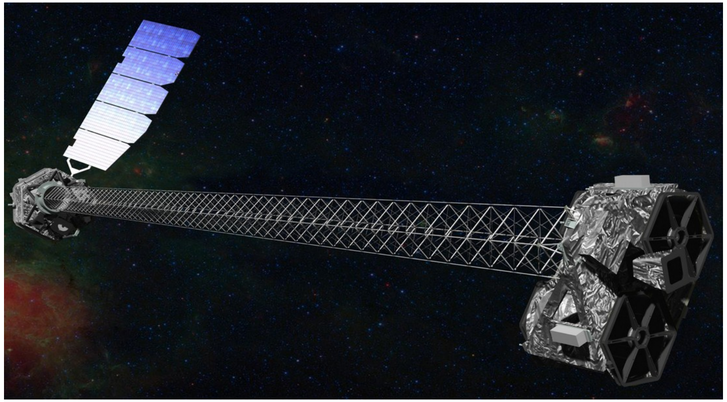

## VERITAS

- Array of four 12m-diameter IACTs
- Energy range: 85 GeV to 30 TeV
- Field of view ~3.5°
- Angular resolution ~0.08° at 1 TeV
- Sensitivity of 1% Crab in < 25h

# Observations and Data Analysis

**Observations summary**

| | NuSTAR | | VERITAS | |
|---|---|---|---|---|
| | date | exposure | date | exposure |
| Nov. 2017 | 22th | 49.7 ks | 16th – 26th | 7.4 hrs |
| Dec. 2017 | 14th | 49.6 ks | 14th – 16th | 6.0 hrs |

**NuSTAR's Legacy Program** **VERITAS' LTP**

**X-ray Timing Analysis**

No evidence of red noise or pulsation was found.

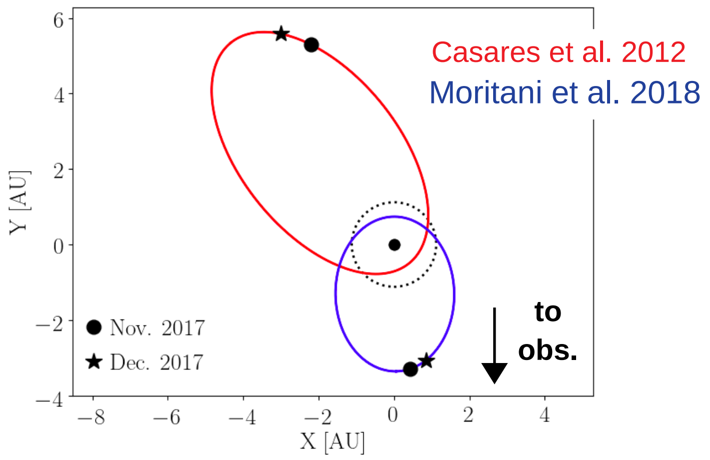


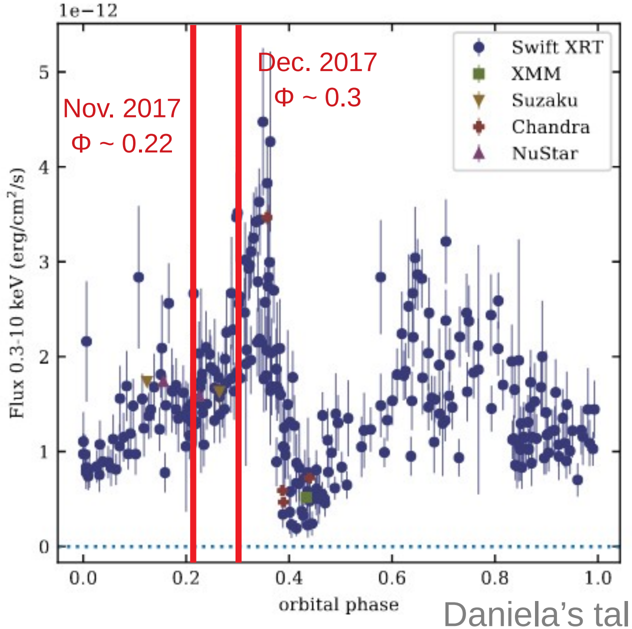


Daniela's talk

# Observations and Data Analysis

NuSTAR →

VERITAS →

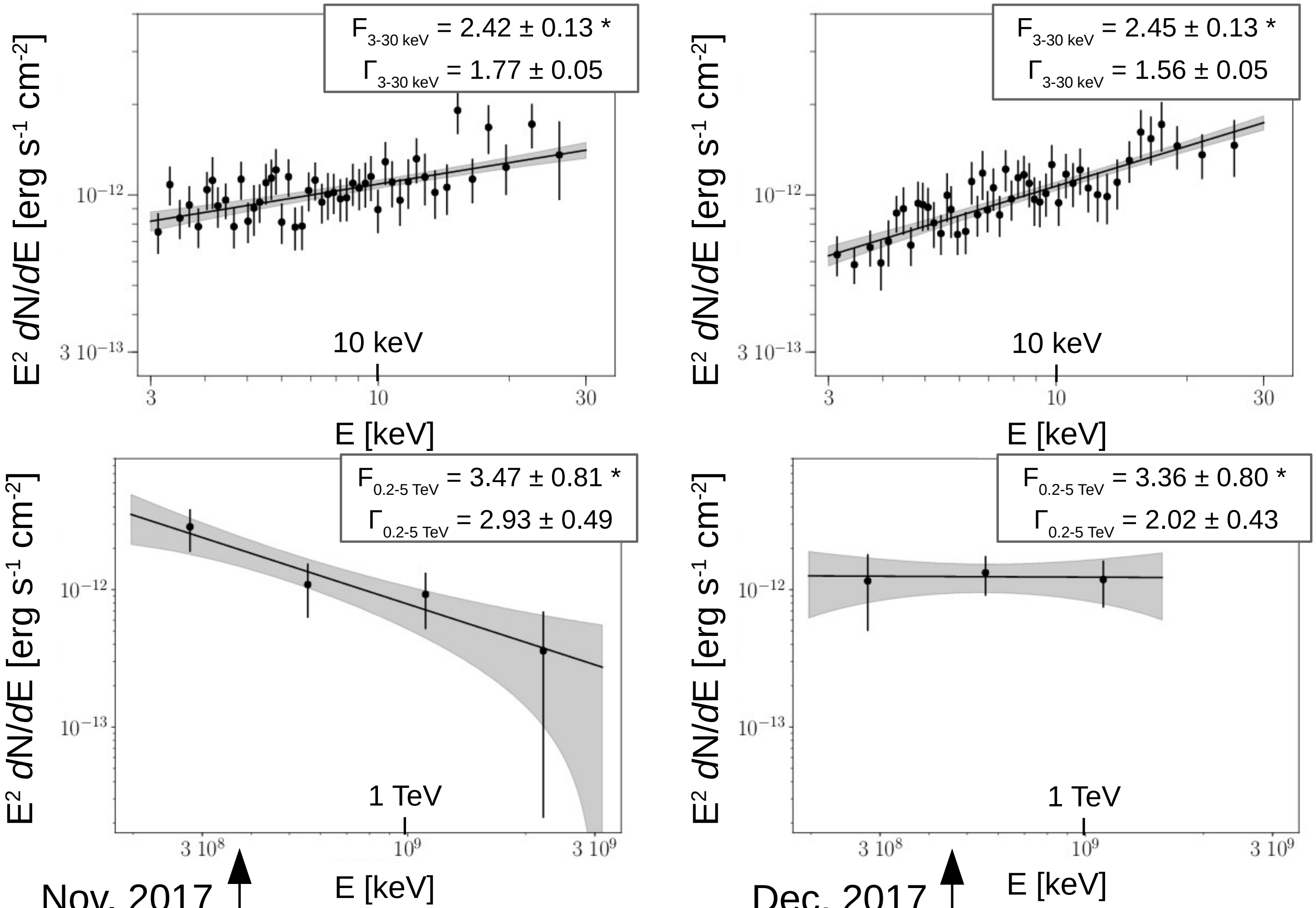


Nov. 2017 ↑

Dec. 2017 ↑

* fluxes in units of $10^{-12}$ erg/$cm^2$/s

# Observations and Data Analysis

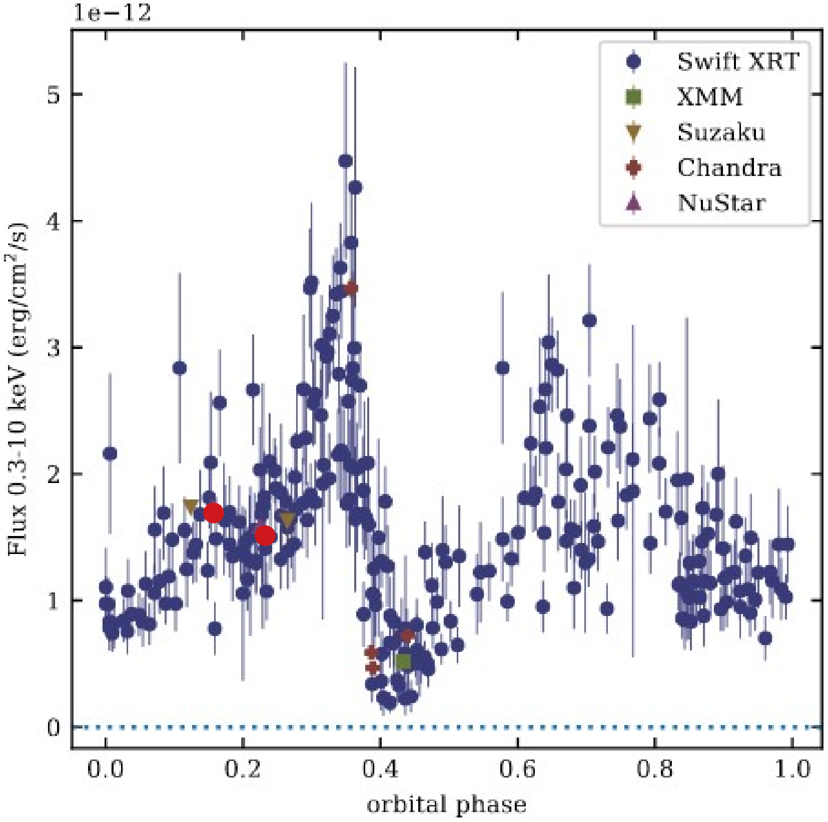


Daniela's talk

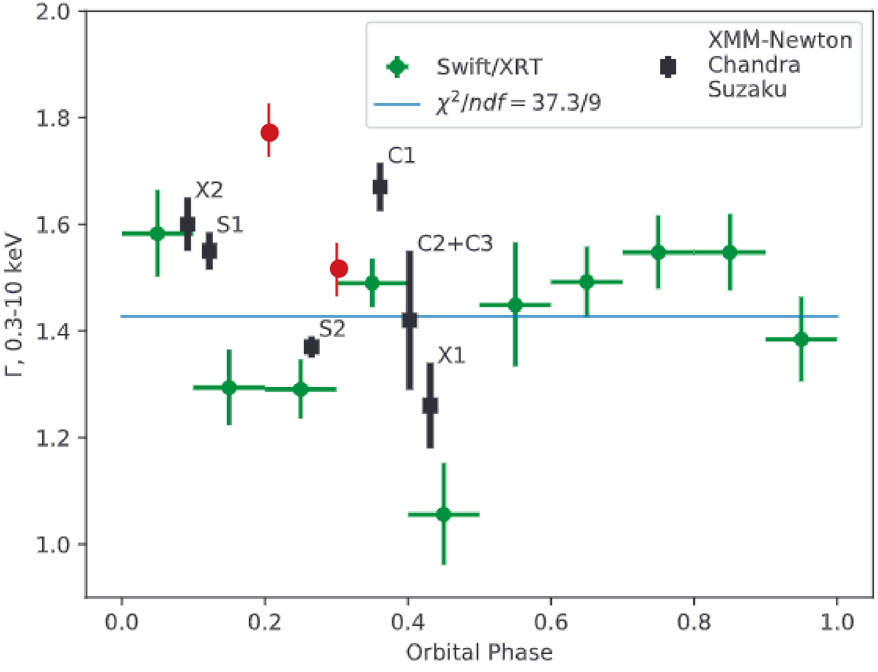


D. Malyshev et al. 2019

# System Parameters and Orbital Solutions

| | Casares et al. 2012 | Moritani et al. 2018 |
|---|---|---|
| $e$ | $0.83 \pm 0.08$ | $0.64 \pm 0.29$ |
| $\omega$ (°) | $129 \pm 17$ | $271 \pm 29$ |
| $f$ ($M_\odot$) | 0.01 | 0.0024 |
| $i$ (°) | $69.5 \pm 10.5$ | $37 \pm 5$ |
| $a_2$ (AU) | $3.90^{+0.13}_{-0.22}$ | $2.13^{+0.14}_{-0.17}$ |
| $P_{\rm orb}$ (d) | $315 \pm 2$ | |
| $M_{\rm psr}$ ($M_\odot$) | 1.4 | |
| $M_{\rm Be}$ ($M_\odot$) | 13.2 – 19.0 | |
| $R_{\rm Be}$ ($R_\odot$) | 7.8 | |
| $T_{\rm Be}$ (K) | 30000 | |
| $v_{\rm w}$ (km/s) | 1500 | |
| $\dot{M}_{\rm w}$ ($M_\odot$/yr) | $10^{8.5\pm0.5}$ | |

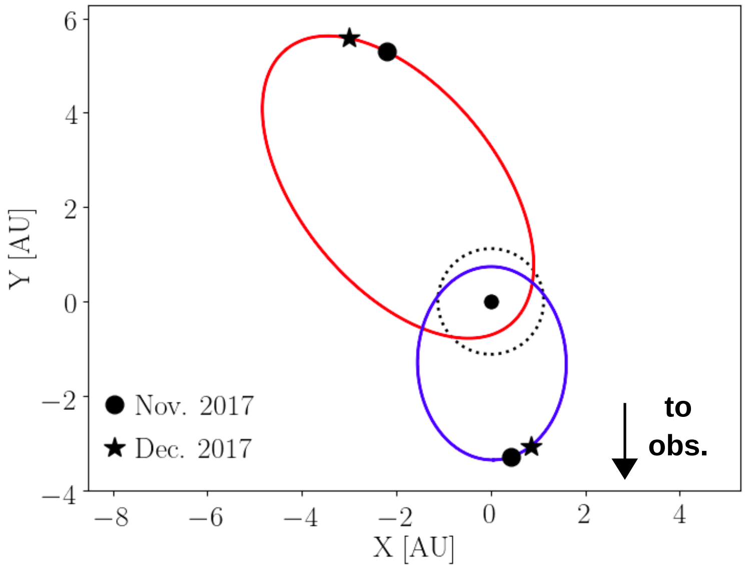

# System Parameters and Orbital Solutions

| | Casares et al. 2012 | Moritani et al. 2018 |
|---|---|---|
| $e$ | $0.83 \pm 0.08$ | $0.64 \pm 0.29$ |
| $\omega$ (°) | $129 \pm 17$ | $271 \pm 29$ |
| $f$ ($M_\odot$) | 0.01 | 0.0024 |
| $i$ (°) | $69.5 \pm 10.5$ | $37 \pm 5$ |
| $a_2$ (AU) | $3.90^{+0.13}_{-0.22}$ | $2.13^{+0.14}_{-0.17}$ |
| $P_{\rm orb}$ (d) | $315 \pm 2$ | |
| $M_{\rm psr}$ ($M_\odot$) | 1.4 | |
| $M_{\rm Be}$ ($M_\odot$) | 13.2 – 19.0 | |
| $R_{\rm Be}$ ($R_\odot$) | 7.8 | |
| $T_{\rm Be}$ (K) | 30000 | |
| $v_{\rm w}$ (km/s) | 1500 | |
| $\dot{M}_{\rm w}$ ($M_\odot$/yr) | $10^{8.5\pm0.5}$ | |

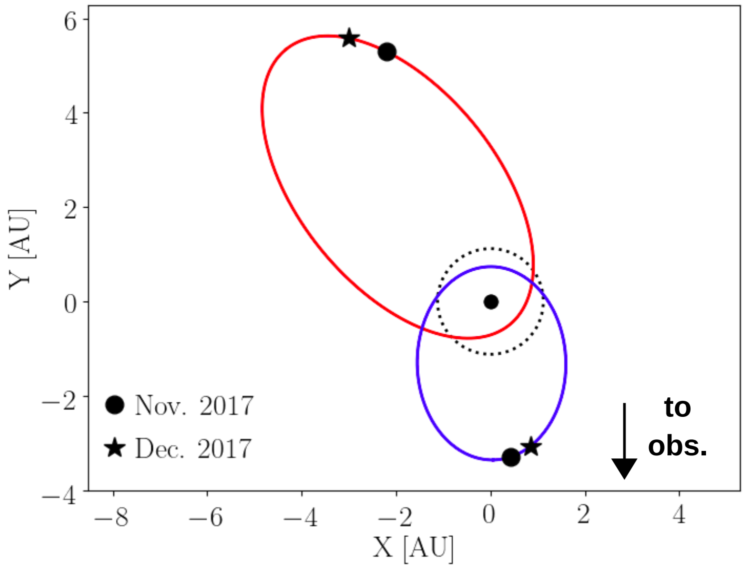


**MWC 148 (HD= 259440)**

Aragona et al. 2010

# System Parameters and Orbital Solutions

| | Casares et al. 2012 | Moritani et al. 2018 |
|---|---|---|
| $e$ | $0.83 \pm 0.08$ | $0.64 \pm 0.29$ |
| $\omega$ (°) | $129 \pm 17$ | $271 \pm 29$ |
| $f$ ($M_\odot$) | 0.01 | 0.0024 |
| $i$ (°) | $69.5 \pm 10.5$ | $37 \pm 5$ |
| $a_2$ (AU) | $3.90^{+0.13}_{-0.22}$ | $2.13^{+0.14}_{-0.17}$ |
| $P_{\rm orb}$ (d) | $315 \pm 2$ | |
| $M_{\rm psr}$ ($M_\odot$) | 1.4 | |
| $M_{\rm Be}$ ($M_\odot$) | $13.2 - 19.0$ | |
| $R_{\rm Be}$ ($R_\odot$) | 7.8 | |
| $T_{\rm Be}$ (K) | 30000 | |
| $v_{\rm w}$ (km/s) | 1500 | |
| $\dot{M}_{\rm w}$ ($M_\odot$/yr) | $10^{8.5\pm0.5}$ | |

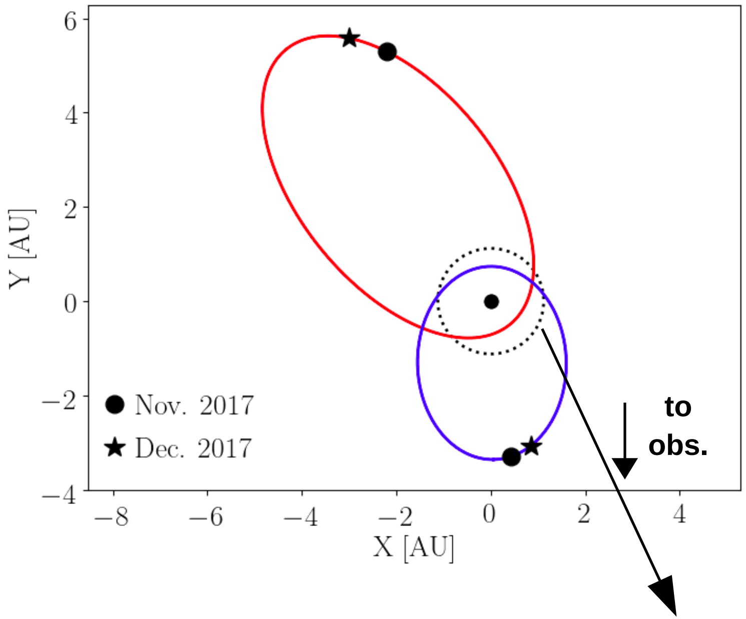


disk component of the stellar wind can be neglected

Moritani et al. 2015
Zamarov et al. 2016
(disk radius estimations)

**stellar wind**

Snow 1981
Waters et al. 1988

# System Parameters and Orbital Solutions

| | Casares et al. 2012 | Moritani et al. 2018 |
|---|---|---|
| $e$ | $0.83 \pm 0.08$ | $0.64 \pm 0.29$ |
| $\omega$ (°) | $129 \pm 17$ | $271 \pm 29$ |
| $f$ ($M_\odot$) | 0.01 | 0.0024 |
| $i$ (°) | $69.5 \pm 10.5$ | $37 \pm 5$ |
| $a_2$ (AU) | $3.90^{+0.13}_{-0.22}$ | $2.13^{+0.14}_{-0.17}$ |
| $P_{\rm orb}$ (d) | $315 \pm 2$ | |
| $M_{\rm psr}$ ($M_\odot$) | 1.4 | |
| $M_{\rm Be}$ ($M_\odot$) | 13.2 – 19.0 | |
| $R_{\rm Be}$ ($R_\odot$) | 7.8 | |
| $T_{\rm Be}$ (K) | 30000 | |
| $v_{\rm w}$ (km/s) | 1500 | |
| $\dot{M}_{\rm w}$ ($M_\odot$/yr) | $10^{8.5\pm0.5}$ | |

**orbital period**

Aliu et al. 2014
(VERITAS+HESS)

# System Parameters and Orbital Solutions

| | Casares et al. 2012 | Moritani et al. 2018 |
|---|---|---|
| $e$ | $0.83 \pm 0.08$ | $0.64 \pm 0.29$ |
| $\omega$ (°) | $129 \pm 17$ | $271 \pm 29$ |
| $f$ ($M_\odot$) | 0.01 | 0.0024 |
| $i$ (°) | $69.5 \pm 10.5$ | $37 \pm 5$ |
| $a_2$ (AU) | $3.90^{+0.13}_{-0.22}$ | $2.13^{+0.14}_{-0.17}$ |
| $P_{\rm orb}$ (d) | $315 \pm 2$ | |
| $M_{\rm psr}$ ($M_\odot$) | 1.4 | |
| $M_{\rm Be}$ ($M_\odot$) | 13.2 – 19.0 | |
| $R_{\rm Be}$ ($R_\odot$) | 7.8 | |
| $T_{\rm Be}$ (K) | 30000 | |
| $v_{\rm w}$ (km/s) | 1500 | |
| $\dot{M}_{\rm w}$ ($M_\odot$/yr) | $10^{8.5 \pm 0.5}$ | |

**compact object is a pulsar (model assumption)**

# System Parameters and Orbital Solutions

## orbital solutions

| | Casares et al. 2012 | Moritani et al. 2018 |
|---|---|---|
| $e$ | $0.83 \pm 0.08$ | $0.64 \pm 0.29$ |
| $\omega$ (°) | $129 \pm 17$ | $271 \pm 29$ |
| $f$ ($M_\odot$) | 0.01 | 0.0024 |
| $i$ (°) | $69.5 \pm 10.5$ | $37 \pm 5$ |
| $a_2$ (AU) | $3.90^{+0.13}_{-0.22}$ | $2.13^{+0.14}_{-0.17}$ |
| $P_{\rm orb}$ (d) | $315 \pm 2$ | |
| $M_{\rm psr}$ ($M_\odot$) | 1.4 | |
| $M_{\rm Be}$ ($M_\odot$) | 13.2 – 19.0 | |
| $R_{\rm Be}$ ($R_\odot$) | 7.8 | |
| $T_{\rm Be}$ (K) | 30000 | |
| $v_{\rm w}$ (km/s) | 1500 | |
| $\dot{M}_{\rm w}$ ($M_\odot$/yr) | $10^{8.5 \pm 0.5}$ | |

## mass function

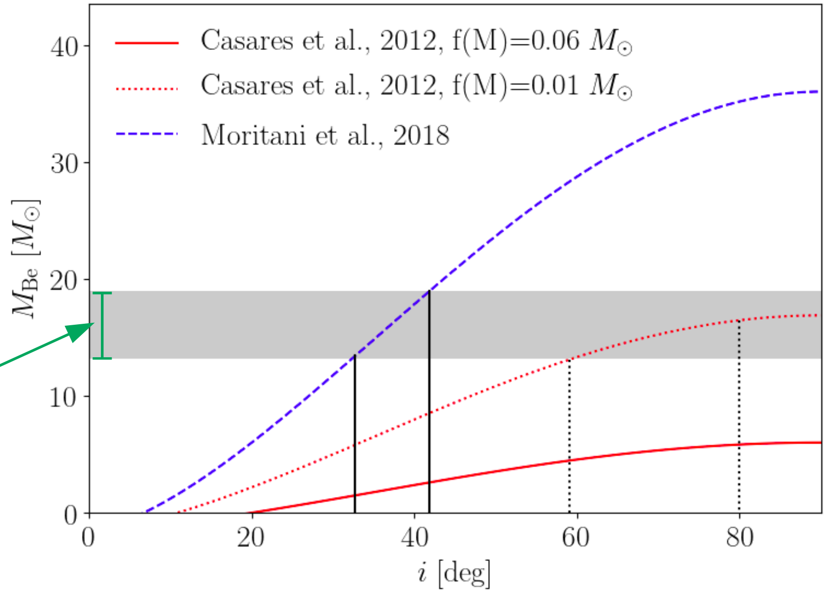


From Casares et al. 2012
f(M) = $0.06^{+0.15}_{-0.05}$ $M_o$

f(M) = 0.01 $M_o$

Inconsistent with the pulsar scenario

Consistent with the pulsar scenario with $59^o < i < 80^o$

# System Parameters and Orbital Solutions

## orbital solutions

| | Casares et al. 2012 | Moritani et al. 2018 |
|---|---|---|
| $e$ | $0.83 \pm 0.08$ | $0.64 \pm 0.29$ |
| $\omega$ (°) | $129 \pm 17$ | $271 \pm 29$ |
| $f$ ($M_\odot$) | 0.01 | 0.0024 |
| $i$ (°) | $69.5 \pm 10.5$ | $37 \pm 5$ |
| $a_2$ (AU) | $3.90^{+0.13}_{-0.22}$ | $2.13^{+0.14}_{-0.17}$ |
| $P_{\rm orb}$ (d) | $315 \pm 2$ | |
| $M_{\rm psr}$ ($M_\odot$) | 1.4 | |
| $M_{\rm Be}$ ($M_\odot$) | 13.2 – 19.0 | |
| $R_{\rm Be}$ ($R_\odot$) | 7.8 | |
| $T_{\rm Be}$ (K) | 30000 | |
| $v_{\rm w}$ (km/s) | 1500 | |
| $\dot{M}_{\rm w}$ ($M_\odot$/yr) | $10^{8.5\pm0.5}$ | |

## mass function

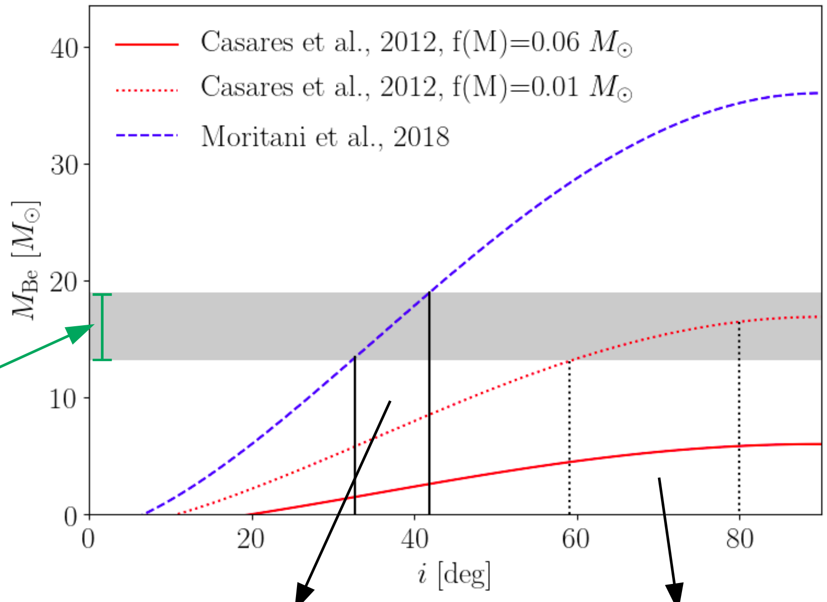


$32^o < i < 42^o$

$59^o < i < 80^o$

# System Parameters and Orbital Solutions

### orbital solutions

| | Casares et al. 2012 | Moritani et al. 2018 |
|---|---|---|
| $e$ | $0.83 \pm 0.08$ | $0.64 \pm 0.29$ |
| $\omega$ (°) | $129 \pm 17$ | $271 \pm 29$ |
| $f$ ($M_\odot$) | 0.01 | 0.0024 |
| $i$ (°) | $69.5 \pm 10.5$ | $37 \pm 5$ |
| $a_2$ (AU) | $3.90^{+0.13}_{-0.22}$ | $2.13^{+0.14}_{-0.17}$ |
| $P_{\rm orb}$ (d) | $315 \pm 2$ | |
| $M_{\rm psr}$ ($M_\odot$) | 1.4 | |
| $M_{\rm Be}$ ($M_\odot$) | 13.2 – 19.0 | |
| $R_{\rm Be}$ ($R_\odot$) | 7.8 | |
| $T_{\rm Be}$ (K) | 30000 | |
| $v_{\rm w}$ (km/s) | 1500 | |
| $\dot{M}_{\rm w}$ ($M_\odot$/yr) | $10^{8.5\pm0.5}$ | |

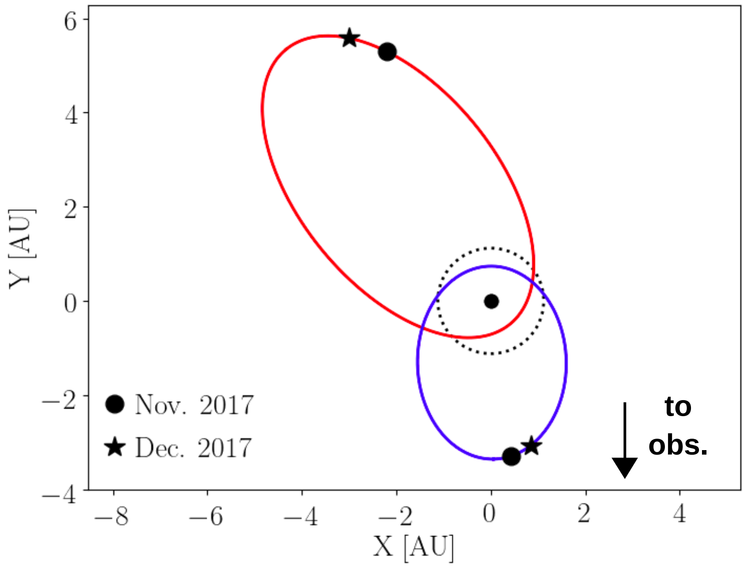

# System Parameters and Orbital Solutions

distance between objects

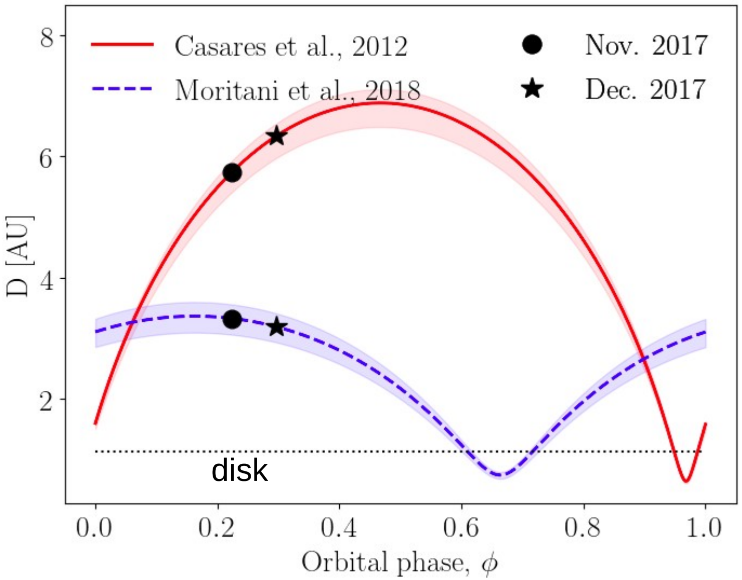


IC scattering angle

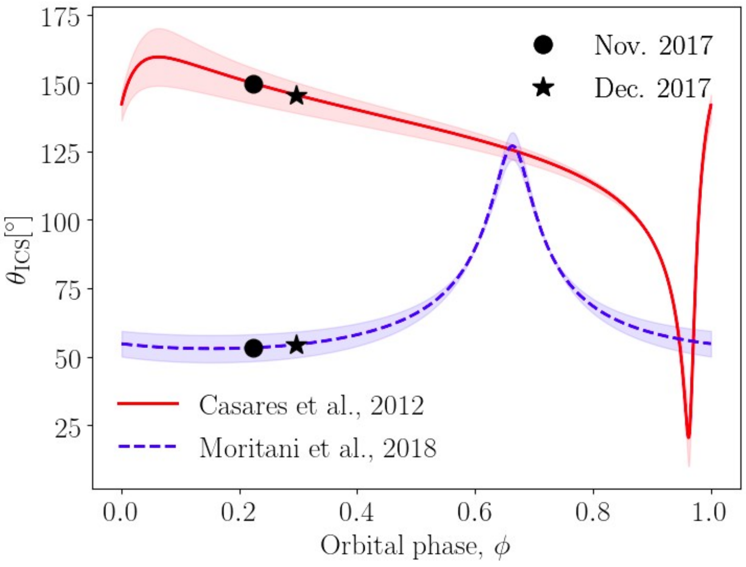


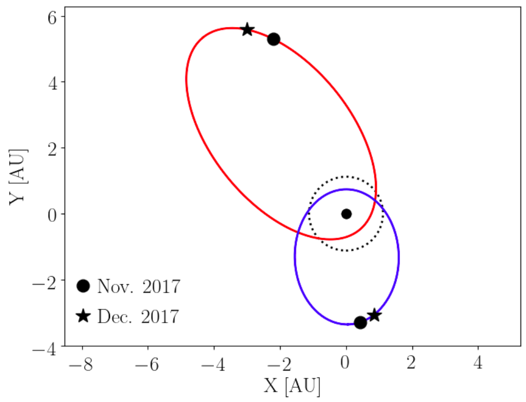


filled band → inclination uncertanties

**32º < i < 42º**

**59º < i < 80º**

# Modeling: Description of the Model

**Main idea:** Pulsar and stellar wind collide and are terminated. Electron pairs from the pulsar wind are accelerated at the **pulsar-wind termination shock** and emit though **synchrotron** and **inverse Compton scattering (ICS)**, producing the observed X-rays and TeV gamma-rays. Stellar photons provide the low energy photons for the ICS.

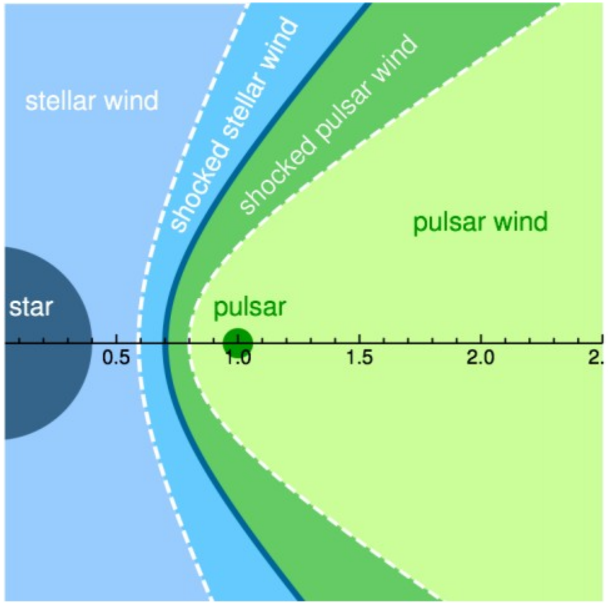


Szostec & Dubus 2011

Tavani & Arons 1997 (PSR B1259-63)

Ball & Kirk 2000

Sierpowska-Bartosik & Torres 2008 (LS 5039)

Takata & Taam 2009 (PSR B1259-63)

Kong et al. 2012 (PSR B1259-63)

Takata et al. 2017 (PSR J2032+4127)

# Modeling: Description of the Model

## Shock Formation and the Pulsar-Wind Magnetization

From the balance between pulsar and stellar wind pressures:

$$R_{\rm sh} = \frac{\sqrt{\eta}}{1+\sqrt{\eta}} D, \quad \eta = \frac{L_{\rm sd}}{\dot{M} v_{\rm w} c}$$

- $R_{\rm sh}$: shock distance from the pulsar
- $D$: distance between stars (obtained from orbital solutions)
- $L_{\rm sd}$: pulsar spin-down luminosity
- $\dot{M} v_{\rm w} c$: stellar wind properties (disk is neglected)

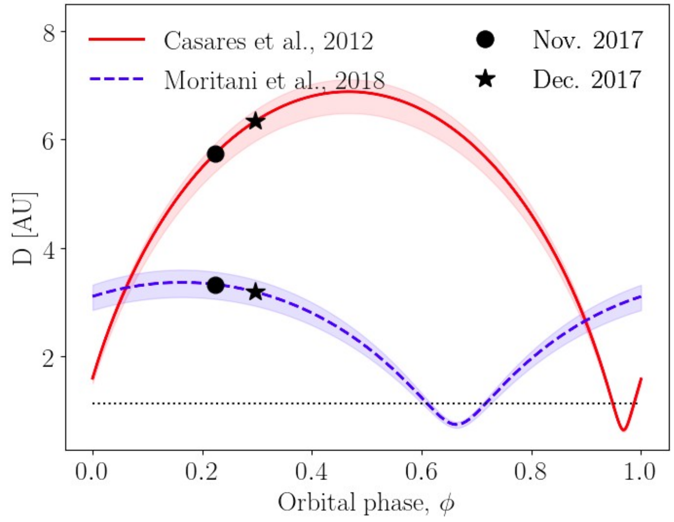


Magnetic field upstream the shock:

$$B = \sqrt{\frac{L_{\rm sd}\sigma}{R_{\rm sh} c (1+\sigma)} \left(1 + \frac{1}{u^2}\right)}$$

- $\sigma$: pulsar-wind magnetization at the shock position

Kennel & Coriniti 1984a, b

# Modeling: Description of the Model

## Energy Spectrum of the High-Energy Electron Population

$$\mathrm{d}N_e/\mathrm{d}E_e = N_e\,(E_e/1\ \mathrm{TeV})^{\Gamma}$$

Single power-law in the range 0.1 – 5 TeV.
(Large overlap at the electron energies responsible for hard X-rays and TeV gamma-rays)

No feature is assumed. A break may exist at < 0.1 TeV and a cut-off may exist at > 5 TeV.

Two free parameters to be fitted ($N_e$ and $\Gamma$).
Injected spectrum and energy losses are not modeled explicitly.

# Modeling: Description of the Model

## Radiative Processes

→ X-rays produced by synchrotron

→ Gamma-rays produced by ICS

- photon field from stellar thermal emission
- anisotropic emission
- pair-production absorption

dependence on orbital solutions (geometry)

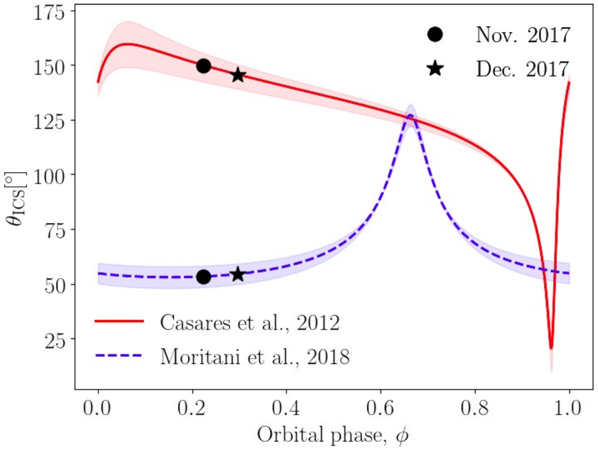


## Model Fitting

→ Combined fit of both periods.

(Nov → index 0, Dec. → index 1)

→ σ scale with $R_{sh}$ as a power law, with α = 1

$$\sigma_1 = \sigma_0 \left( \frac{R_{sh,0}}{R_{sh,1}} \right)^{\alpha}$$

→ Slope of electron spectra computed from X-rays SED fit of single power law.

→ 4 free parameters: $\mathbf{L_{sd}}$, **σ**, $\mathbf{N_{e,0}}$ **and** $\mathbf{N_{e,1}}$

→ $\chi^2$ minimization method

# Modeling: Results

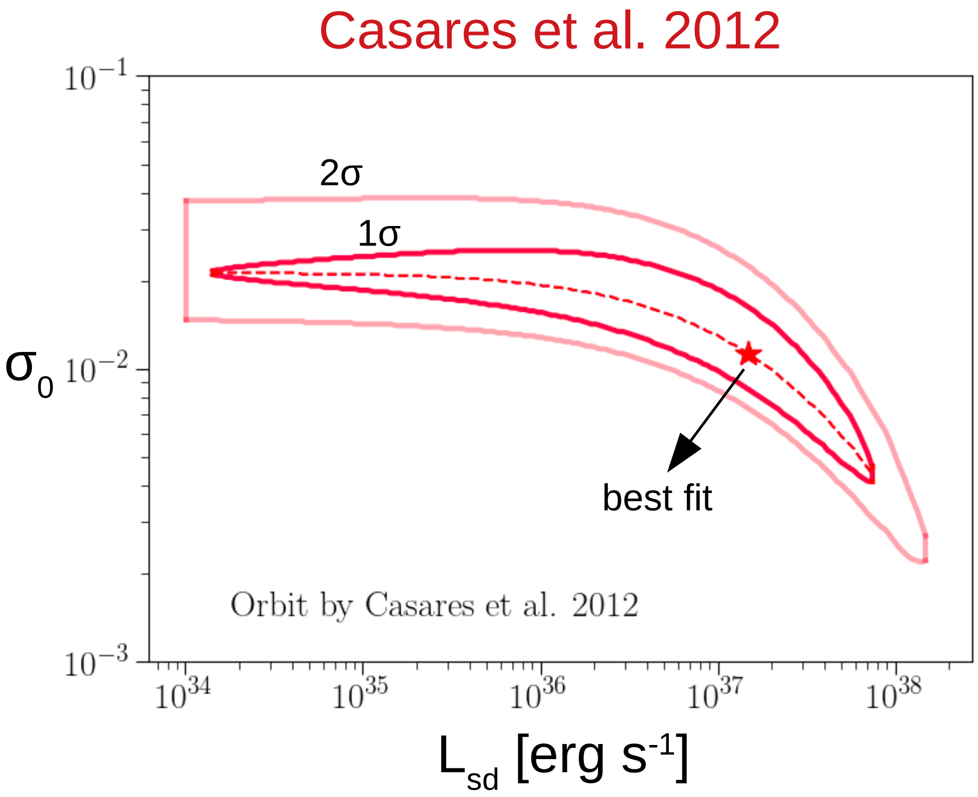


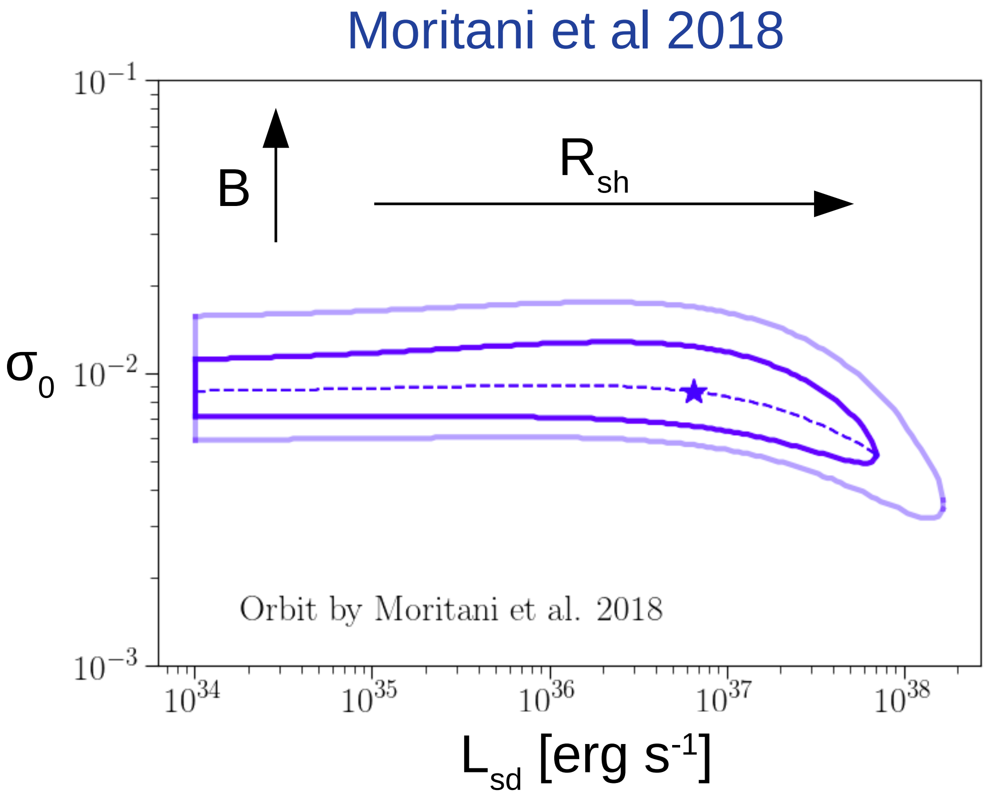

# Modeling: Results

## Fitted SEDs for the best fit solution

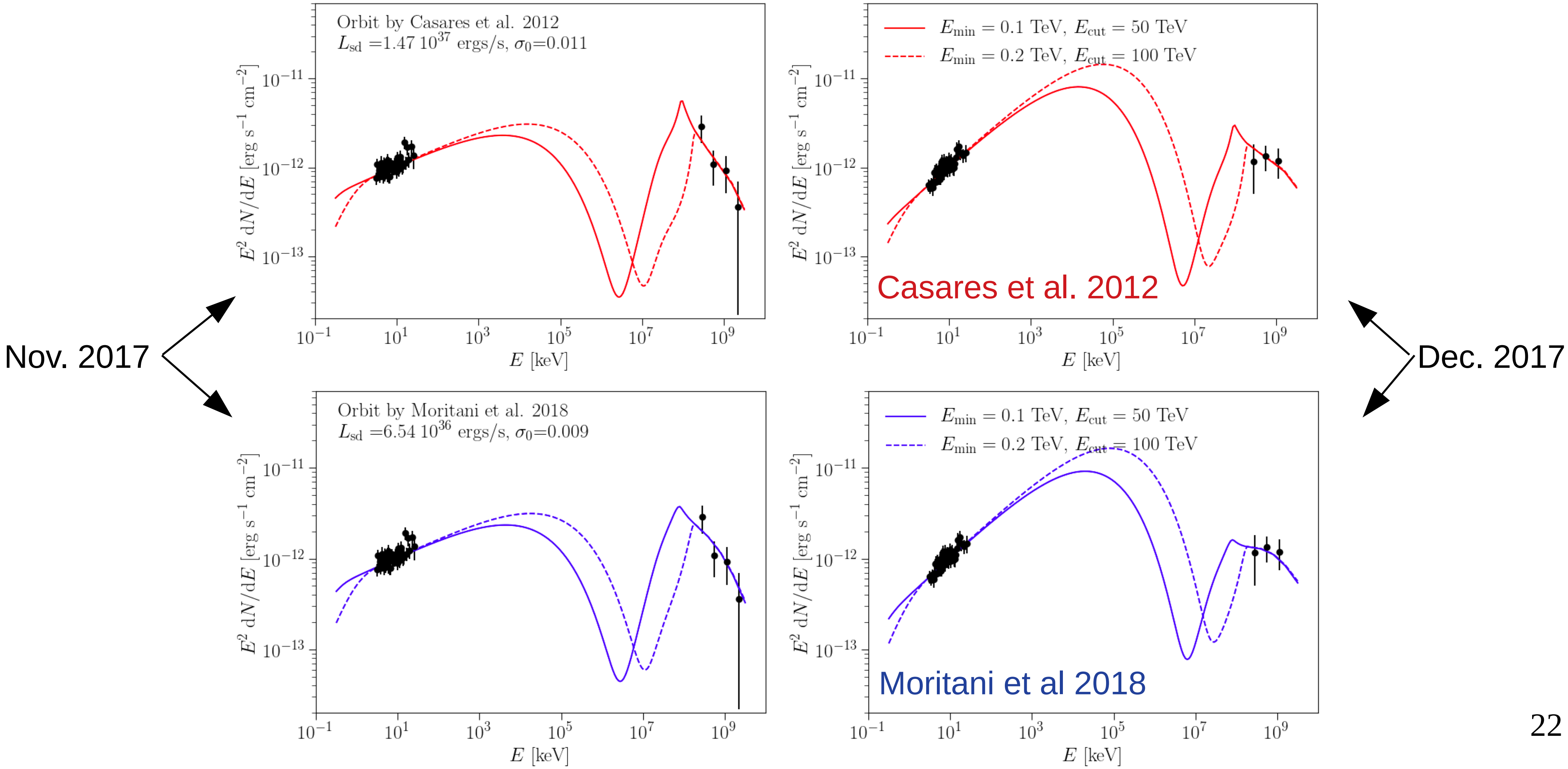

# Modeling: Results

Casares et al. 2012

Moritani et al 2018

magnetic field | shock distance | g-g optical depth

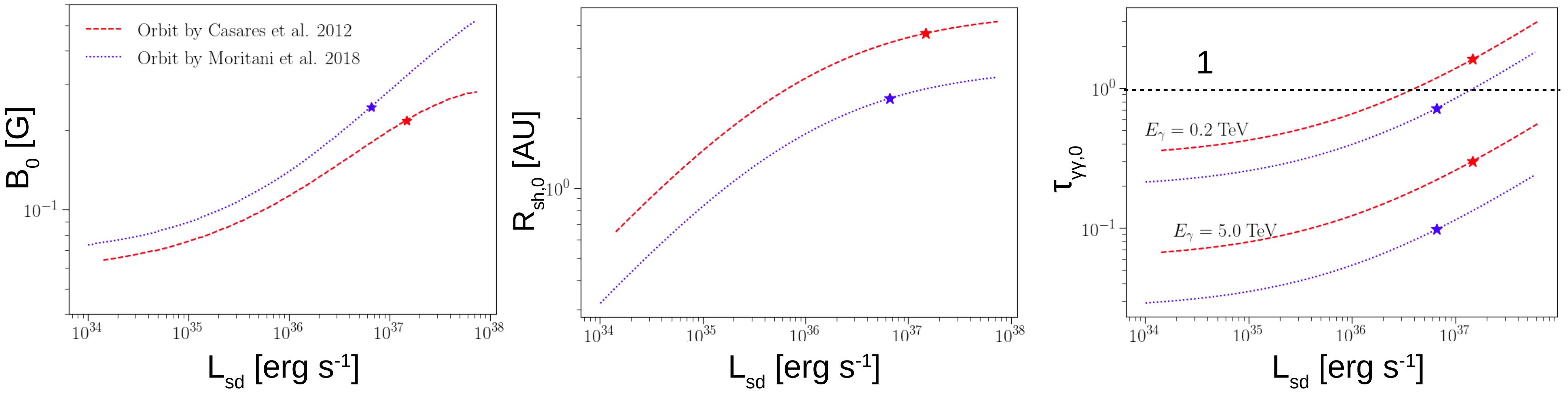

# Modeling: Results

Casares et al. 2012
Moritani et al 2018

$10^{-9}$ < mass loss rate [$M_o$/yr] < $10^{-8}$

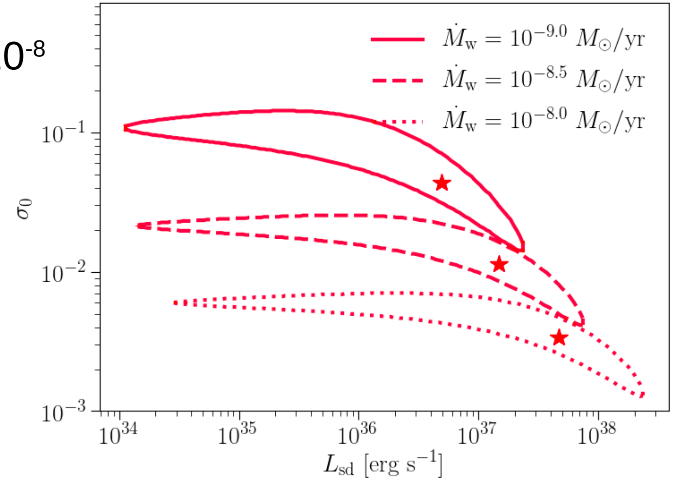


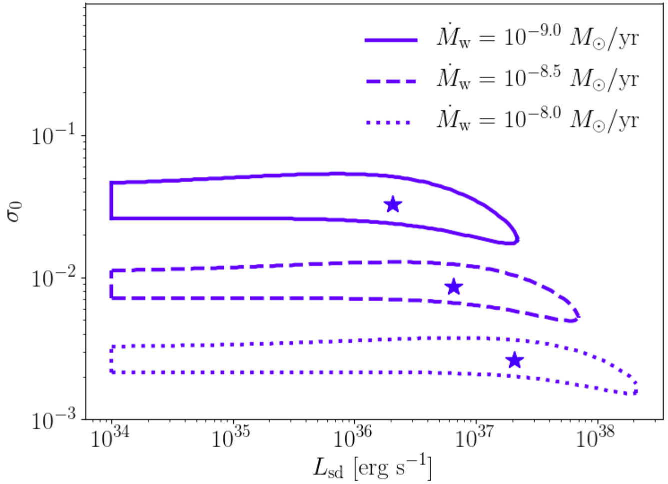


**32º < i < 42º**

**59º < i < 80º**

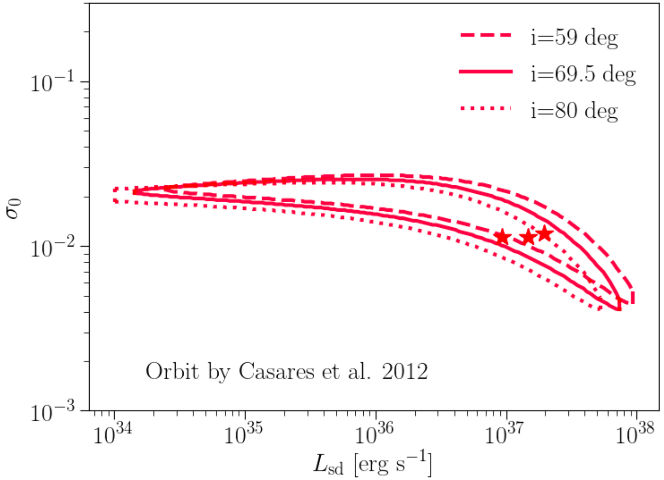


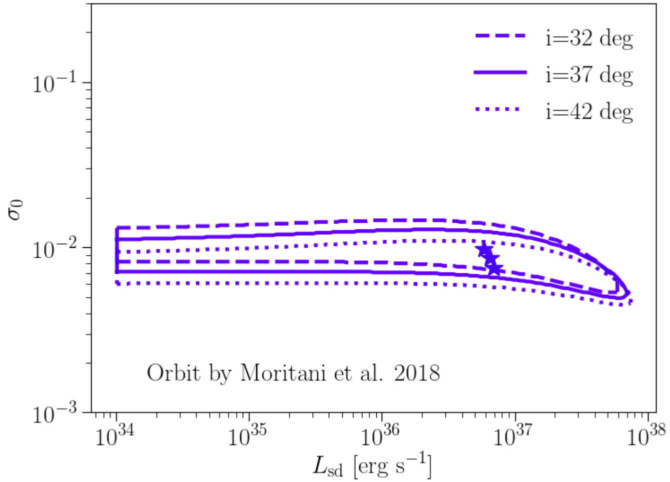

# Modeling: Results

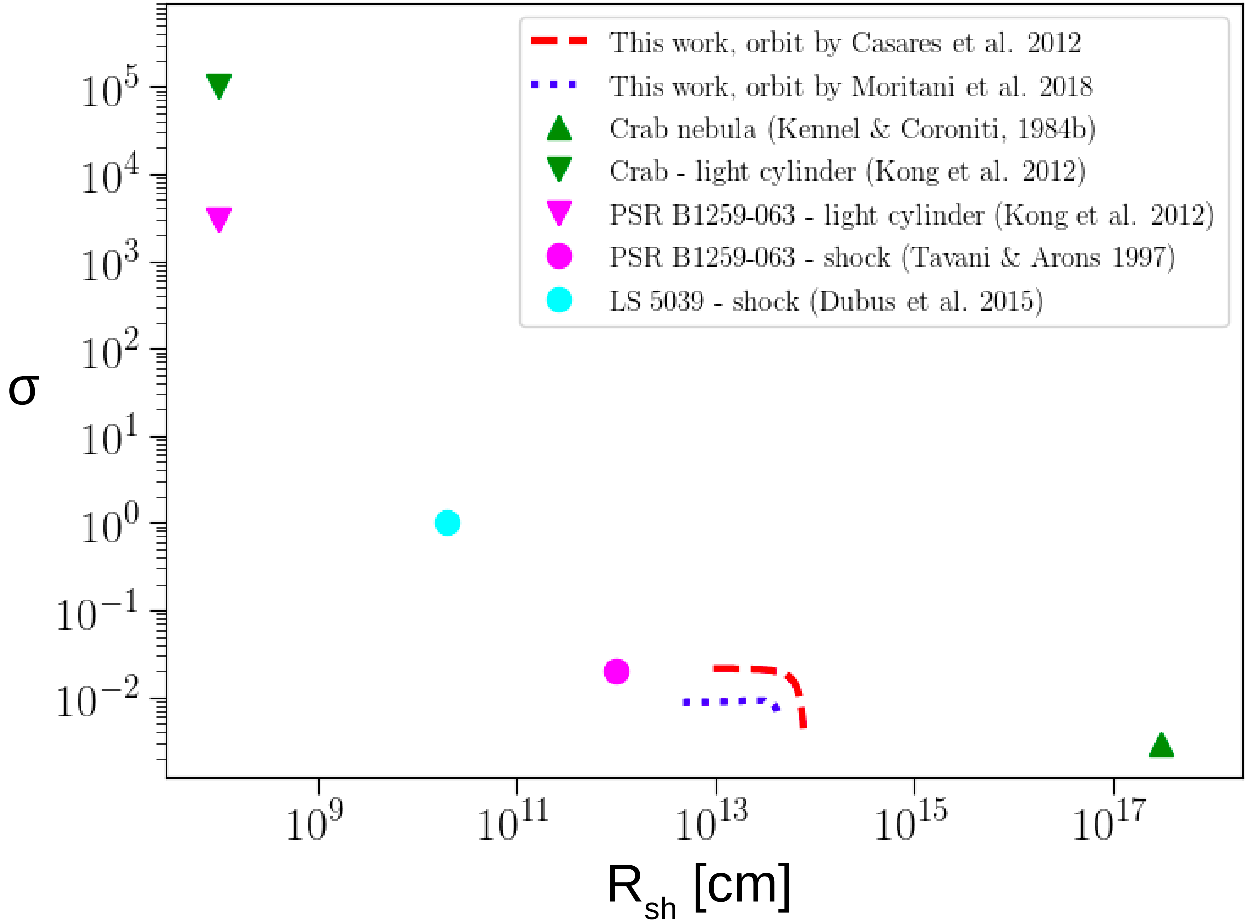

# Modeling: Results

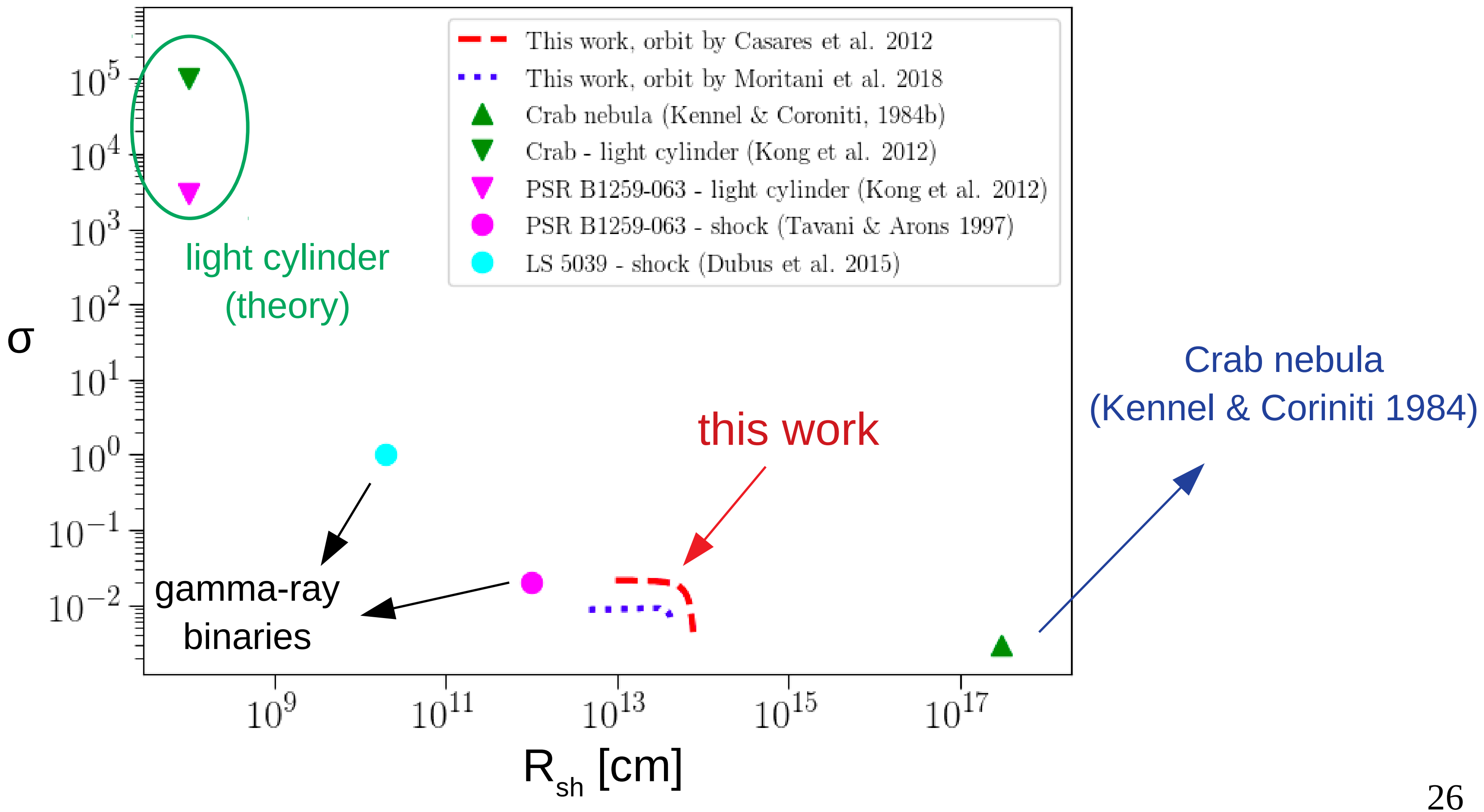

# Summary and Conclusions

**Observations**

- Two sets of combined observations by VERITAS and NuSTAR
- First observations in hard X-rays
- No evidence of red noise or pulsation in X-rays

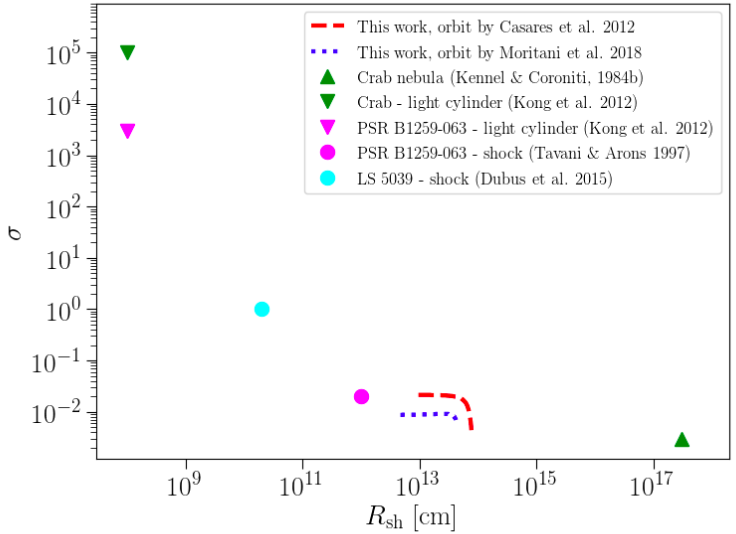


**Modeling**

- SED data properly described within the pulsar scenario
- Model with minimum assumptions
- Constraints on the pulsar-wind magnetization

**Future**

- Combined NuSTAR + VERITAS observations in the 2019/2020 cycle

# Thank you!